

## Absolute photoneutron cross sections for Zr, I, Pr, Au, and Pb

B. L. Berman

*Department of Physics, The George Washington University, Washington, D.C. 20052*

R. E. Pywell

*Saskatchewan Accelerator Laboratory, University of Saskatchewan, Saskatoon, Saskatchewan, Canada S7N 0W0*

S. S. Dietrich

*Lawrence Livermore National Laboratory, University of California, Livermore, California 94550*

M. N. Thompson

*School of Physics, University of Melbourne, Parkville, Victoria, Australia 3052*

K. G. McNeill

*Department of Physics, University of Toronto, Toronto, Ontario, Canada M5S 1A7*

J. W. Jury

*Department of Physics, Trent University, Peterborough, Ontario, Canada K9J 7B8*

(Received 21 May 1987)

The photoneutron cross sections for  $^{nat}\text{Zr}$ ,  $^{127}\text{I}$ ,  $^{141}\text{Pr}$ ,  $^{197}\text{Au}$ , and  $^{nat}\text{Pb}$  have been measured near the peak of the giant dipole resonance, with monoenergetic photons, in such a way that the absolute cross sections for these nuclei were intercalibrated, using  $^{141}\text{Pr}$  as a benchmark. The measured peak total photoneutron cross sections are, within an uncertainty of 2–3%, 174, 252, 340, 502, and 602 mb for  $^{nat}\text{Zr}$ ,  $^{127}\text{I}$ ,  $^{141}\text{Pr}$ ,  $^{197}\text{Au}$ , and  $^{nat}\text{Pb}$ , respectively. These results resolve outstanding discrepancies among previous measurements.

### I. MOTIVATION AND METHOD

Over the years, the photoneutron cross sections for many nuclei have been measured with monoenergetic photons at the Lawrence Livermore National Laboratory and at the Centre d'Etudes Nucléaires de Saclay: 82 at Livermore and 99 at Saclay. In addition, 13 nuclei have been measured at the laboratories at General Atomic, Pennsylvania, Illinois, and Giessen. All these data are presented in Ref. 1. For most of the cases studied, the agreement among the results of these laboratories is remarkably good. The case of  $^{141}\text{Pr}$ , which was studied at no fewer than four of these laboratories, is notable. At Livermore, the photoneutron cross sections for this nucleus were measured twice before, in 1966 (Ref. 2) and 1974;<sup>3,4</sup> at General Atomic, in 1970;<sup>5</sup> at Saclay, in 1971;<sup>6</sup> and at Illinois, in 1972.<sup>7</sup> However, there are a few cases where appreciable discrepancies still exist. Among these are  $^{90}\text{Zr}$ ,<sup>8,9</sup>  $^{127}\text{I}$ ,<sup>2,10</sup> and  $^{208}\text{Pb}$ ,<sup>11,12</sup> where the Livermore and Saclay results disagree in peak height by  $\sim 15\%$  or more. The cross section for  $^{208}\text{Pb}$  measured at Illinois<sup>7</sup> agrees with that from Saclay.<sup>12</sup> In the case of  $^{197}\text{Au}$ , the Livermore and Saclay cross sections<sup>13,12</sup> agree in peak height but not in width.

In order to clear up these outstanding discrepancies, we have remeasured the photoneutron cross sections for the five nuclei mentioned above across the peak of the giant dipole resonance. The  $^{141}\text{Pr}$  sample was included

as a test case because of the excellent agreement between the results of the five previous monoenergetic-photon measurements.

The method used was the same as has been used before at Livermore, and is documented in Refs. 1 and 14 and elsewhere. The measurements reported here were carried out at the same time as the  $^{14}\text{C}(\gamma, n)$  measurements reported in Ref. 15. The solid samples were in the form of right circular cylinders of natural elements having masses of approximately 100 g each. It should be noted that the isotopic abundances of  $^{90}\text{Zr}$  in the  $^{nat}\text{Zr}$  sample and of  $^{208}\text{Pb}$  in the  $^{nat}\text{Pb}$  sample are 51.5% and 52.4%, respectively; the other elements are monoisotopic. The energy range of the measurements extends above the  $(\gamma, 2n)$  thresholds for certain isotopes. Table I lists the sample masses, the energy range of the measured data, and the  $(\gamma, 2n)$  threshold energies.

The most noteworthy feature of the experimental method, for the present purposes, is the use of a remotely controlled pneumatic eight-position revolving sample changer, which allowed all of the samples, as well as a blank sample and a neutron calibration source, to be inserted sequentially into the center of the  $4\pi$  neutron detector without changing the beam tuning or any other experimental conditions. This feature enabled us to make relative cross-section measurements with a precision of  $\sim 2\%$ , much better than the overall absolute accuracy of  $\sim 5\%$  typical of recent measurements near

TABLE I. Sample properties.

Sample	Mass (g)	$E_{\gamma\min}$ (MeV)	$E_{\gamma\max}$ (MeV)	$E_{\text{thr}}(\gamma,2n)$ (MeV)
$^{\text{nat}}\text{Zr}$	113.4	14.9	19.7	14.9 (for $^{94}\text{Zr}$ ) <sup>a</sup>
$^{127}\text{I}$	100.0	12.1	16.9	16.2
$^{141}\text{Pr}$	100.2	12.1	16.9	17.3
$^{197}\text{Au}$	126.5	12.1	16.9	14.8
$^{\text{nat}}\text{Pb}$	99.7	12.1	16.9	14.1 (for $^{208}\text{Pb}$ )

<sup>a</sup>21.3 MeV for  $^{90}\text{Zr}$ .

the peak of the giant resonance of medium and heavy nuclei.

## II. EXPERIMENTAL RESULTS

The photoneutron cross sections for  $^{\text{nat}}\text{Zr}$ ,  $^{127}\text{I}$ ,  $^{141}\text{Pr}$ ,  $^{197}\text{Au}$ , and  $^{\text{nat}}\text{Pb}$  measured here are shown in Figs. 1–5,

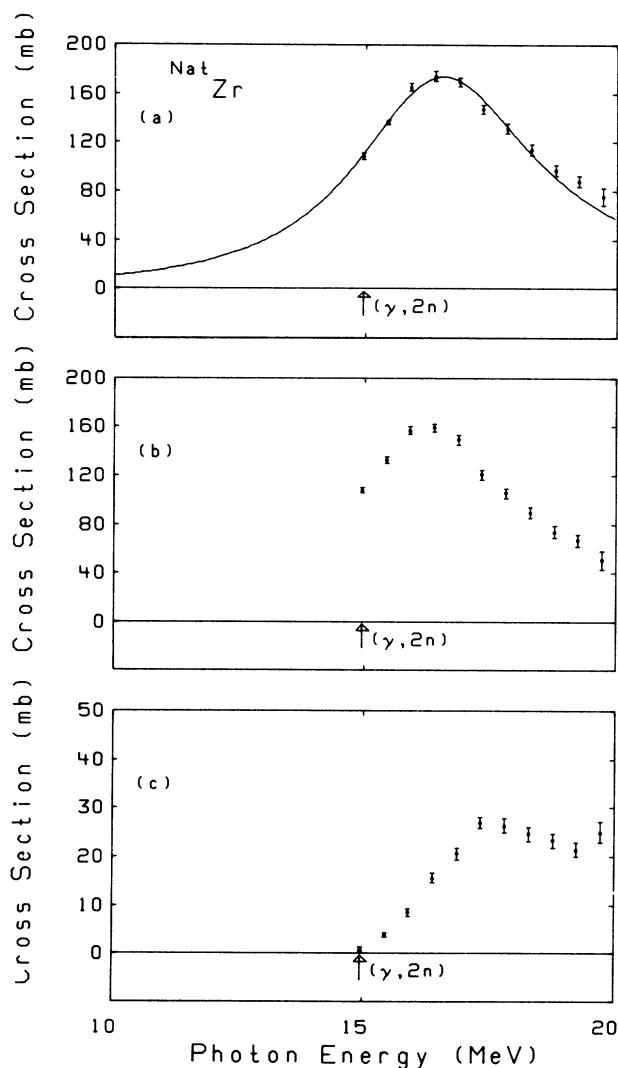


FIG. 1. Measured photoneutron cross sections for  $^{\text{nat}}\text{Zr}$ : (a)  $\sigma(\gamma, n_{\text{tot}}) = \sigma(\gamma, 1n) + \sigma(\gamma, 2n)$ ; (b)  $\sigma(\gamma, 1n)$ ; and (c)  $\sigma(\gamma, 2n)$ . The best-fit Lorentz curve to  $\sigma(\gamma, n_{\text{tot}})$  also is shown in part (a). Thresholds are indicated by arrows.

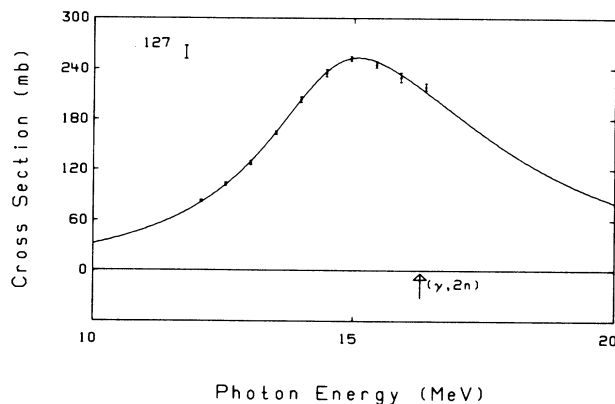


FIG. 2. Measured total photoneutron cross section for  $^{127}\text{I}$ , with the best-fit (two-component) Lorentz curve.

respectively. The total photoneutron cross section is the sum of the single- and double-photon cross sections,  $\sigma(\gamma, n_{\text{tot}}) = \sigma(\gamma, 1n) + \sigma(\gamma, 2n)$ , as distinct from the photoneutron yield cross section  $\sigma(\gamma, \text{Sn}) = \sigma(\gamma, 1n) + 2\sigma(\gamma, 2n)$ . The  $(\gamma, 2n)$  threshold for  $^{141}\text{Pr}$  lies higher in energy than the measured data, so that only the  $(\gamma, 1n)$  cross section, which is the same as the total photoneutron cross section  $\sigma(\gamma, n_{\text{tot}})$  below the  $(\gamma, 2n)$  threshold, is shown in Fig. 3. For  $^{127}\text{I}$ , because only two of the data points lie higher than the  $(\gamma, 2n)$  threshold [for these two points,  $\sigma(\gamma, 2n) = 2.1 \pm 1.1$  mb at 16.4 MeV and  $21.4 \pm 1.7$  mb at 16.9 MeV], again only  $\sigma(\gamma, n_{\text{tot}})$  is shown in Fig. 2. For the others, the data extend above the  $(\gamma, 2n)$  threshold of at least one isotope contained in the elemental samples, and for these cases  $\sigma(\gamma, n_{\text{tot}})$ ,  $\sigma(\gamma, 1n)$ ,  $\sigma(\gamma, 2n)$  are shown separately, as parts (a), (b), and (c), respectively, of Figs. 1, 4, and 5. The integrated  $(\gamma, 2n)$  cross sections up to  $E_{\gamma\max}$  (see Table I) for  $^{\text{nat}}\text{Zr}$ ,  $^{197}\text{Au}$ , and  $^{\text{nat}}\text{Pb}$  are 88, 116, and 145 MeV mb, respectively.

## III. COMPARISON WITH OLDER DATA

The main interest here is the comparison of the present cross-section data, particularly their absolute magnitudes, with the older data in the literature.

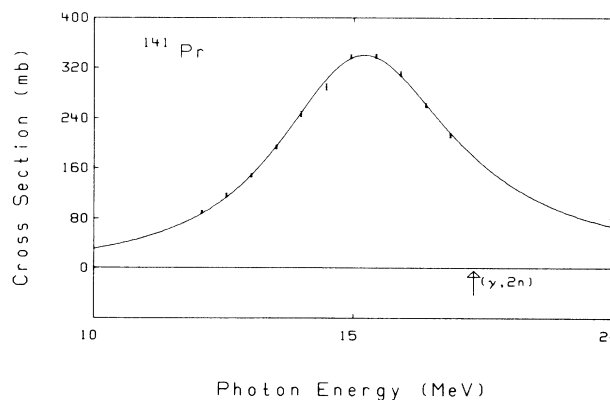


FIG. 3. Measured total photoneutron cross section for  $^{141}\text{Pr}$ , with the best-fit Lorentz curve.

A.  $^{141}\text{Pr}$ 

The fact that the  $^{141}\text{Pr}$  nucleus would be suitable as a benchmark for photoneutron data was noted in Ref. 14. The total photoneutron cross section for  $^{141}\text{Pr}$  as measured in the present work is shown in Fig. 6, this time with the Lorentz curve that represents the average of the five previous data sets for this nucleus (see below). There is very little difference between this curve and the one in Fig. 3. All of the sets of  $^{141}\text{Pr}$  data, in the form of the parameters of Lorentz curves fitted to the data (using the same least-squares fitting procedure and for the same fitting intervals, from Ref. 1), are compared in Table II. They are all in very good agreement with each other, the largest deviation from the mean absolute magnitude being 4%. Also given in Table II are the average Lorentz parameters for the five previous measurements. The agreement between the present data and these average

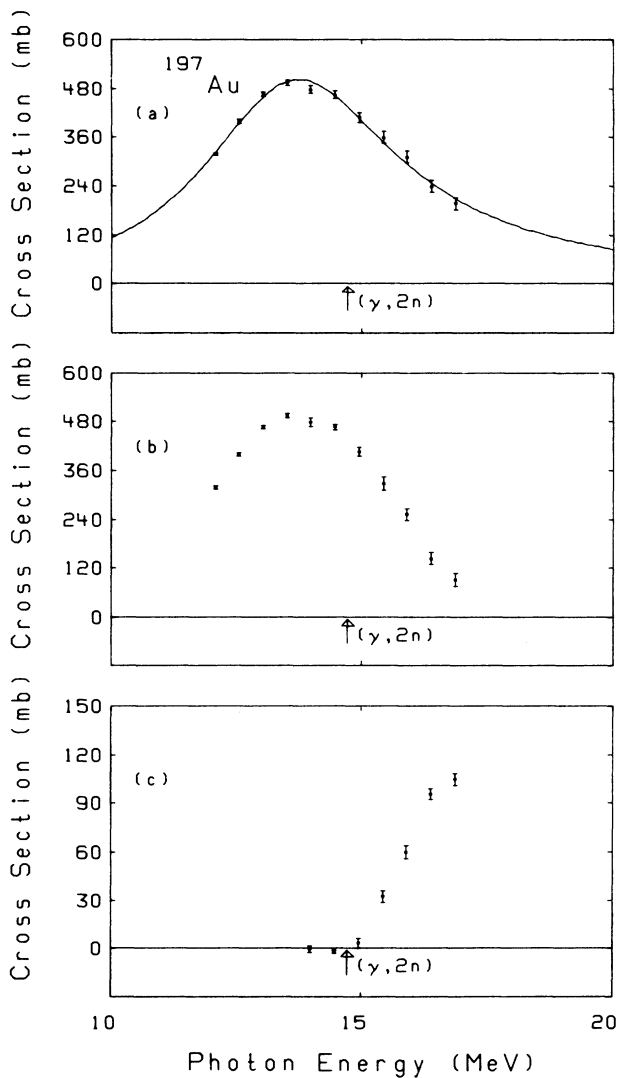


FIG. 4. Measured photoneutron cross sections for  $^{197}\text{Au}$ ; (a)  $\sigma(\gamma, n_{\text{tot}})$ , together with the best-fit Lorentz curve; (b)  $\sigma(\gamma, 1n)$ ; and (c)  $\sigma(\gamma, 2n)$ .

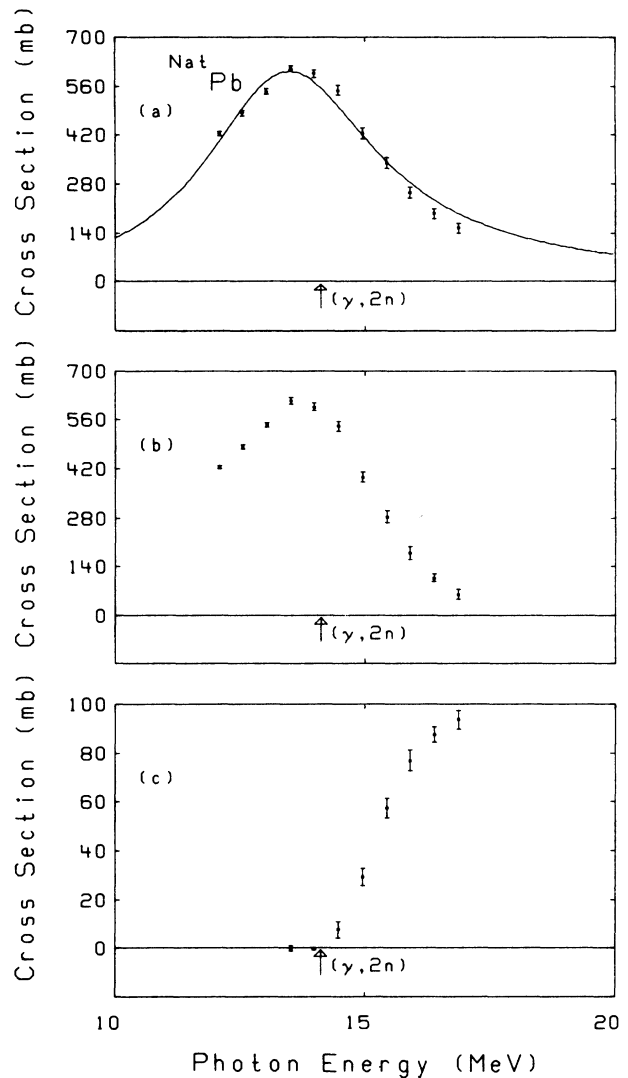


FIG. 5. Measured photoneutron cross sections for  $^{\text{nat}}\text{Pb}$ ; (a)  $\sigma(\gamma, n_{\text{tot}})$ , together with the best-fit Lorentz curve; (b)  $\sigma(\gamma, 1n)$ ; and (c)  $\sigma(\gamma, 2n)$ .

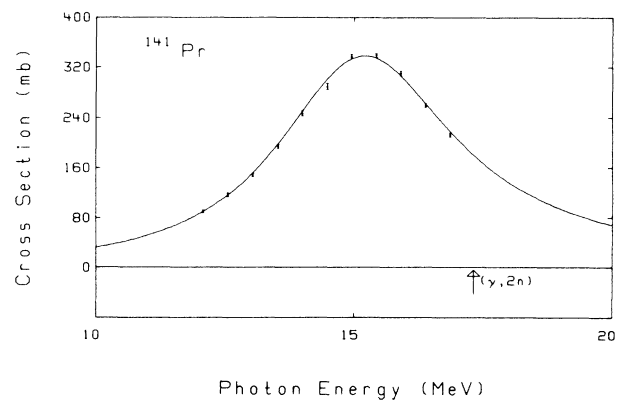


FIG. 6.  $\sigma(\gamma, n_{\text{tot}})$  for  $^{141}\text{Pr}$ , with the Lorentz curve whose parameters are the average of the five previous data sets (Refs. 2-7).

TABLE II. Comparison of data for  $^{141}\text{Pr}$ .

Data set	$E_m$ (MeV)	$\sigma_m$ (mb)	$\Gamma$ (MeV)	Date	Reference	Figure number
Livermore I	15.15	324	4.42	1966	2	
General Atomic	15.23	341	4.00	1970	5	
Saclay	15.04	347	4.49	1971	6	
Illinois	15.36	332	4.07	1972	7	
Livermore II	15.19	344	4.24	1974	3 and 4	
Average of the above	15.19	338	4.24	1966-74	2-7	6
Livermore III	15.19	340	4.15		Present data	3

parameters is superb (0.6% in magnitude). Thus, the present cross sections for  $^{\text{nat}}\text{Zr}$ ,  $^{127}\text{I}$ ,  $^{197}\text{Au}$ , and  $^{\text{nat}}\text{Pb}$  should be as accurate in absolute magnitude (within 2-3 %) as that for  $^{141}\text{Pr}$ .

### B. $^{\text{nat}}\text{Zr}$

The total photoneutron cross section for  $^{\text{nat}}\text{Zr}$  is shown in Fig. 7, this time with a Lorentz curve for  $^{\text{nat}}\text{Zr}$  reconstructed from the separated-isotope data of Ref. 8. The parameters of this curve are given in Table III; the natural isotopic abundances are used as weighting factors. [Because  $^{96}\text{Zr}$  (whose natural abundance is 2.8%) was not measured by the authors of Ref. 8, we follow their procedure and assume its total cross section to be the same as that for  $^{94}\text{Zr}$  (whose abundance is 17.4%) for purposes of this analysis.] Again, there is excellent agreement (within 1.7% in magnitude), between the Livermore data of 1967 (Ref. 8) and the present Livermore data. As in the case of  $^{141}\text{Pr}$ , there is very little difference between the two curves in Figs. 1 and 7.

Comparison of the Livermore and Saclay data of Refs. 8 and 9 shows that for  $^{90}\text{Zr}$ , the magnitude of the peak cross section from Saclay is 14% higher than that from Livermore, and for  $^{89}\text{Y}$  the Saclay peak cross section is 22% higher. For both of these cases the  $(\gamma, 2n)$  threshold lies above the fitting interval for the giant-resonance

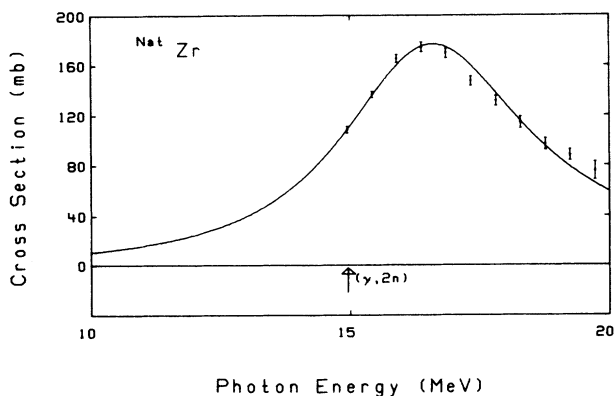


FIG. 7.  $\sigma(\gamma, n_{\text{tot}})$  for  $^{\text{nat}}\text{Zr}$ , with a Lorentz curve reconstructed from the separated-isotope data of Ref. 8.

data, so that neutron-multiplicity counting is not at issue here (see Sec. IV). Therefore, this comparison implies an error either in the photon flux determination or in the neutron detection efficiency or in both. We therefore recommend that the Livermore cross sections for  $^{90}\text{Zr}$ ,  $^{91}\text{Zr}$ ,  $^{92}\text{Zr}$ ,  $^{94}\text{Zr}$ , and also  $^{89}\text{Y}$  (all measured at the same time) be accepted. For the same reasons, we recommend that the Saclay cross sections for  $^{\text{nat}}\text{Rb}$ ,  $^{\text{nat}}\text{Sr}$ ,  $^{89}\text{Y}$ ,  $^{90}\text{Zr}$ , and  $^{93}\text{Nb}$  (all from Ref. 9) be reduced by  $18 \pm 4\%$ . [We also note that the Illinois data for  $^{89}\text{Y}$  (Ref. 7) lie midway between the Livermore and Saclay results.]

This recommendation has a significant impact on the

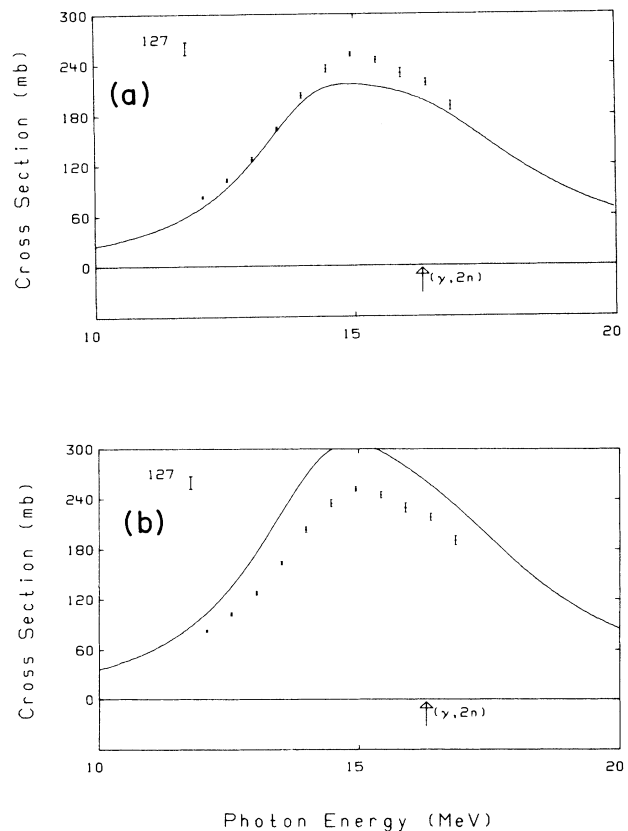


FIG. 8.  $\sigma(\gamma, n_{\text{tot}})$  for  $^{127}\text{I}$ , with the best-fit (two-component) Lorentz curve to the data of (a) Ref. 2 and (b) Ref. 10.

TABLE III. Lorentz parameters for  $^{nat}\text{Zr}$ .

Isotope	Natural abundance (%)	$E_m$ (MeV)	$\sigma_m$ (mb)	$\Gamma$ (MeV)	Reference	Figure number
$^{90}\text{Zr}$	51.5	16.85	185	4.02	8	
$^{91}\text{Zr}$	11.2	16.58	184	4.20	8	
$^{92}\text{Zr}$	17.1	16.26	166	4.68	8	
$^{94}\text{Zr}$	20.2 <sup>a</sup>	16.22	161	5.29	8	
$^{nat}\text{Zr}$	100	16.59	177	4.41	From data in 8	7
$^{nat}\text{Zr}$	100	16.52	174	4.41	Present data	1

<sup>a</sup>Sum of abundances of  $^{94}\text{Zr}$  and  $^{96}\text{Zr}$  (see text).

conclusions of Veysière *et al.* in Ref. 16. If the integrated total photoneutron cross section for  $^{nat}\text{Zr}$  from threshold to 30 MeV is reduced by 18%, the integrated total *photonuclear* cross section up to 140 MeV is reduced by 9%, and the enhancement factor  $\mathcal{H}$ , where  $\sigma_{\text{int}} = \sigma_{\text{TRK}}(1 + \mathcal{H})$  ( $\sigma_{\text{TRK}}$  is the Thomas-Reiche-Kuhn sum-rule value), is reduced by 25%, from 0.73 to 0.57.

### C. $^{127}\text{I}$

The total photoneutron cross section for  $^{127}\text{I}$  is shown in Fig. 8, together with two (two-component) Lorentz curves, (a) the best fit to the old Livermore data of Ref. 2 and (b) the best fit to the Saclay data of Ref. 10. It is

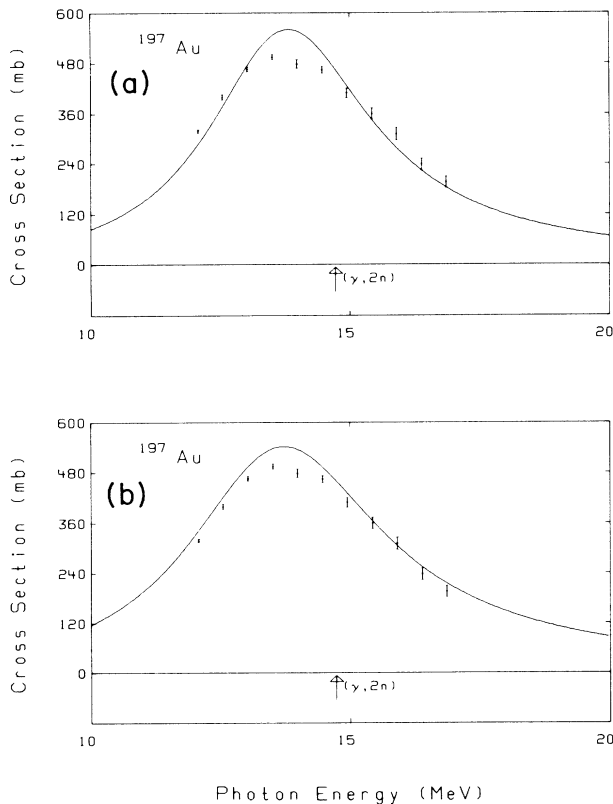


FIG. 9.  $\sigma(\gamma, n_{\text{tot}})$  for  $^{197}\text{Au}$ , with the best-fit Lorentz curves to the data of (a) Ref. 13 and (b) Ref. 12.

immediately evident that in the giant-resonance region the cross section measured at Livermore<sup>2</sup> is too small and has the wrong shape and that measured at Saclay,<sup>10</sup> although consistent in shape with the present data, is too large. We recommend that the best estimate of the cross section be obtained by multiplying the Saclay data by 0.80. We also note that although Ref. 2 reported data on both  $^{141}\text{Pr}$  and  $^{127}\text{I}$ , these two data sets were not obtained at the same time nor analyzed in the same way.

### D. $^{197}\text{Au}$

The total photoneutron cross section for  $^{197}\text{Au}$  is shown in Fig. 9. Two Lorentz curves are shown here as well, the best fits to (a) the older Livermore data of Ref. 13 and (b) the Saclay data of Ref. 12; the parameters of these curves are given in Table IV. It can be seen that both of the older sets, which agree with each other in peak cross section, lie about 10% higher than the present data. Since the Saclay values for the resonance energy and width lie closer to the present values, we recommend that the Saclay total cross section be reduced by about 8%, while the much older Livermore data not be used at all.

### E. $^{nat}\text{Pb}$

The total photoneutron cross section for  $^{nat}\text{Pb}$  is shown in Fig. 10, together with a Lorentz curve for  $^{nat}\text{Pb}$

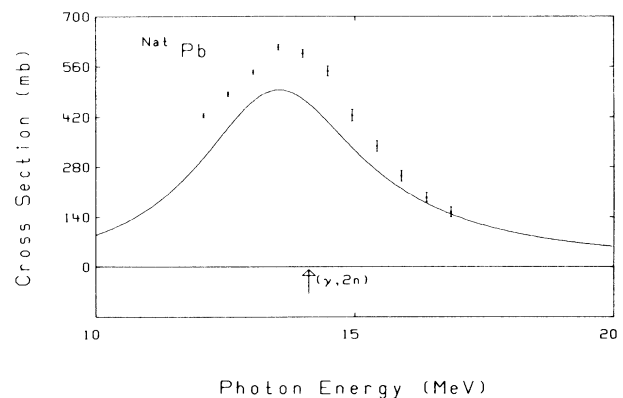


FIG. 10.  $\sigma(\gamma, n_{\text{tot}})$  for  $^{nat}\text{Pb}$ , with a Lorentz curve reconstructed from the separated-isotope data of Ref. 11.

TABLE IV. Lorentz parameters for  $^{197}\text{Au}$ .

Data set	$E_m$ (MeV)	$\sigma_m$ (mb)	$\Gamma$ (MeV)	Date	Reference	Figure number
Livermore I	13.82	560	3.84	1962	13	9
Saclay	13.72	541	4.61	1970	12	9
Livermore II	13.73	502	4.76		Present data	4

reconstructed from the separated-isotope data from Livermore.<sup>11</sup> Since the total cross sections for all three major isotopes of lead are nearly the same,<sup>11</sup> it is clear that the cross sections of Ref. 11 are far too low. The Lorentz parameters of this curve are given in Table V; they show that the total cross sections of Ref. 11 should be increased by 22% to match the present data.

The Lorentz parameters for  $^{208}\text{Pb}$  obtained from the Saclay and Illinois data<sup>12,7</sup> also are given in Table V. These values are much closer to the present ones than are those of Ref. 11. The Saclay data are closest in both peak height and width, the peak height being only 6% greater than that for the present data for  $^{\text{nat}}\text{Pb}$ . Therefore, we recommend that the Saclay cross-section scale for  $^{208}\text{Pb}$  be reduced by about 7%, consistent with our recommendation for  $^{197}\text{Au}$  (the results for  $^{197}\text{Au}$  were also reported in Ref. 12). We also recommend that the old Livermore cross sections for  $^{206}\text{Pb}$ ,  $^{207}\text{Pb}$ ,  $^{208}\text{Pb}$ , and also  $^{209}\text{Bi}$  (all from Ref. 11) be increased by 22%.

This increase in the Livermore cross-section scale for  $^{209}\text{Bi}$  brings it into agreement with the Illinois data<sup>7</sup> for this nucleus; the Livermore peak cross section becomes 634 mb, versus 648 mb from Ref. 7. It also agrees with the value of 646 mb recently inferred by Kahane<sup>17</sup> from an analysis of elastic photon-scattering data for  $^{209}\text{Bi}$ .

#### IV. NEUTRON-MULTIPLICITY COUNTING

Wolynec *et al.*<sup>18</sup> have performed an extensive comparative analysis of the Livermore and Saclay data for medium and heavy nuclei. Of the nuclei discussed above, they have analyzed (among a total of 12) the

cases of  $^{89}\text{Y}$ ,  $^{197}\text{Au}$ , and  $^{208}\text{Pb}$ . They conclude that the neutron-multiplicity-sorting procedure used at Livermore is correct and that the one used at Saclay is not. Can the present data throw light upon this conclusion?

First, this analysis should require that the two ( $\gamma,1n$ ) cross sections below the ( $\gamma,2n$ ) threshold be normalized in order to correct for discrepancies in absolute calibration. Since an absolute calibration error would be most evident at the peak of the giant resonance, the measurements reported here should help to resolve this normalization question. In the case of  $^{89}\text{Y}$ , the analysis of Sec. III indicates that the Saclay data should be multiplied by 0.82 (the Livermore data were multiplied by 1.255 in Ref. 20). For  $^{197}\text{Au}$ , we recommend that the Saclay data be multiplied by 0.93 but that the Livermore data not be used at all. For  $^{208}\text{Pb}$ , we recommend that the Livermore data be multiplied by 1.22 and the Saclay data by 0.93 (the Livermore data were multiplied by 1.296 in Ref. 20). Thus for  $^{89}\text{Y}$  and  $^{208}\text{Pb}$  the *relative* normalizations that would be obtained from the present data are within 3% of the values used in Ref. 20, so that this alone should not affect the conclusions of Ref. 20 very much.

We also have obtained some new ( $\gamma,2n$ ) cross-section data, shown in Figs. 1(c), 4(c), and 5(c). Unfortunately, however, these data extend only up to a few MeV above the ( $\gamma,2n$ ) thresholds and are for multi-isotopic samples except for the case of  $^{197}\text{Au}$ . For this nucleus, our new ( $\gamma,2n$ ) data are nearly the same as the Saclay ( $\gamma,2n$ ) data of Ref. 12. Even after normalizing the Saclay data by the recommended 7%, the two sets of ( $\gamma,2n$ ) data are not sufficiently disparate to enable us to confirm the conclusions of Ref. 20.

TABLE V. Lorentz parameters for  $^{\text{nat}}\text{Pb}$  and  $^{208}\text{Pb}$ .

Isotope	Natural abundance (%)	$E_m$ (MeV)	$\sigma_m$ (mb)	$\Gamma$ (MeV)	Reference	Figure number
$^{206}\text{Pb}$	25.5 <sup>a</sup>	13.59	514	3.85	11	
$^{207}\text{Pb}$	22.1	13.56	481	3.96	11	
$^{208}\text{Pb}$	52.4	13.46	491	3.90	11	
$^{\text{nat}}\text{Pb}$	100	13.52	495	3.90	From data in 11	10
$^{\text{nat}}\text{Pb}$	100	13.48	602	4.20	Present data	5
$^{208}\text{Pb}$	52.4	13.43	639	4.07	12	
$^{208}\text{Pb}$	52.4	13.63	645	3.94	7	

<sup>a</sup>Sum of abundances of  $^{204}\text{Pb}$  (1.4%) and  $^{206}\text{Pb}$  (24.1%).

## V. SUMMARY

We have remeasured the photoneutron cross sections for  $^{nat}\text{Zr}$ ,  $^{127}\text{I}$ ,  $^{141}\text{Pr}$ ,  $^{197}\text{Au}$ , and  $^{nat}\text{Pb}$  across the peak of the giant dipole resonance, with monoenergetic photons from the annihilation in flight of fast positrons from the Lawrence Livermore National Laboratory Electron-Positron Linear Accelerator. The experimental conditions were such that we are confident that these new results can be used to intercalibrate the absolute photoneutron cross sections for these nuclei. The  $^{141}\text{Pr}$  total photoneutron cross section was used as a benchmark because all six measurements of this cross section performed using monoenergetic photons (including the present one) agree to within a few percent. On the basis of the data presented here, we recommend that previously reported results be normalized as specified in Table VI. These new results affect numerous previous conclusions in the literature, on a wide variety of subjects; three of them (see Refs. 16, 17, and 18) have been discussed here.

## ACKNOWLEDGMENTS

The experimental work reported here was performed at Lawrence Livermore National Laboratory under the auspices of the U.S. Department of Energy under Contract No. W-7405-ENG-48. This work was supported as well by the National Sciences and Engineering Council

TABLE VI. Recommended normalization factors.

Isotope	Laboratory	Reference	Normalization factor
$^{nat}\text{Rb}$	Saclay	9	$0.85 \pm 0.03$
$^{nat}\text{Sr}$	Saclay	9	$0.85 \pm 0.03$
$^{89}\text{Y}$	Saclay	9	0.82
$^{89}\text{Y}$	Livermore	8	1.0
$^{90}\text{Zr}$	Saclay	9	0.88
$^{90}\text{Zr}$	Livermore	8	1.0
$^{91}\text{Zr}$	Livermore	8	1.0
$^{92}\text{Zr}$	Livermore	8	1.0
$^{93}\text{Nb}$	Saclay	9	$0.85 \pm 0.03$
$^{94}\text{Zr}$	Livermore	8	1.0
$^{127}\text{I}$	Saclay	10	0.80
$^{127}\text{I}$	Livermore	2	a
$^{197}\text{Au}$	Saclay	12	0.93
$^{197}\text{Au}$	Livermore	13	a
$^{206}\text{Pb}$	Livermore	11	1.22
$^{207}\text{Pb}$	Livermore	11	1.22
$^{208}\text{Pb}$	Livermore	11	1.22
$^{208}\text{Pb}$	Saclay	12	0.93
$^{208}\text{Bi}$	Livermore	11	1.22

<sup>a</sup>Do not use.

of Canada and by the Australian Research Grants Committee. A previous report on part of the material presented here appeared as Ref. 19.

- <sup>1</sup>S. S. Dietrich and B. L. Berman, *At. Data Nucl. Data Tables* (in press).
- <sup>2</sup>R. L. Bramblett, J. T. Caldwell, B. L. Berman, R. R. Harvey, and S. C. Fultz, *Phys. Rev.* **148**, 1198 (1966).
- <sup>3</sup>J. T. Caldwell, E. J. Dowdy, B. L. Berman, R. A. Alvarez, and P. Meyer, *Phys. Rev. C* **21**, 1215 (1980).
- <sup>4</sup>B. L. Berman, J. T. Caldwell, E. J. Dowdy, S. S. Dietrich, P. Meyer, and R. A. Alvarez, *Phys. Rev. C* **34**, 2201 (1986).
- <sup>5</sup>R. E. Sund, V. V. Verbinski, H. Weber, and L. A. Kull, *Phys. Rev. C* **2**, 1129 (1970).
- <sup>6</sup>H. Beil, R. Bergère, P. Carlos, A. Leprêtre, A. Veysière, and A. Parlag, *Nucl. Phys.* **A172**, 426 (1971).
- <sup>7</sup>L. M. Young, Ph.D. thesis, University of Illinois, 1972.
- <sup>8</sup>B. L. Berman, J. T. Caldwell, R. R. Harvey, M. A. Kelly, R. L. Bramblett, and S. C. Fultz, *Phys. Rev.* **162**, 1098 (1967).
- <sup>9</sup>A. Leprêtre, H. Beil, R. Bergère, P. Carlos, A. Veysière, and M. Sugawara, *Nucl. Phys.* **A175**, 609 (1971).
- <sup>10</sup>R. Bergère, H. Beil, P. Carlos, and A. Veysière, *Nucl. Phys.* **A133**, 417 (1969).
- <sup>11</sup>R. R. Harvey, J. T. Caldwell, R. L. Bramblett, and S. C.

Fultz, *Phys. Rev.* **136B**, 126 (1964).

- <sup>12</sup>A. Veysière, H. Beil, R. Bergère, P. Carlos, and A. Leprêtre, *Nucl. Phys.* **A159**, 561 (1970).
- <sup>13</sup>S. C. Fultz, R. L. Bramblett, J. T. Caldwell, and N. A. Kerr, *Phys. Rev.* **127**, 1273 (1962).
- <sup>14</sup>B. L. Berman and S. C. Fultz, *Rev. Mod. Phys.* **47**, 713 (1975).
- <sup>15</sup>R. E. Pywell, B. L. Berman, J. G. Woodworth, J. W. Jury, K. G. McNeill, and M. N. Thompson, *Phys. Rev. C* **32**, 384 (1985).
- <sup>16</sup>A. Veysière, H. Beil, R. Bergère, P. Carlos, J. Fagot, A. Leprêtre, and A. de Miniac, *Z. Phys. A* **306**, 139 (1982).
- <sup>17</sup>S. Kahane, *Phys. Rev. C* **33**, 1793 (1986).
- <sup>18</sup>E. Wolyneec, A. R. V. Martinez, P. Gouffon, Y. Miyão, V. A. Serrão, and M. N. Martins, *Phys. Rev. C* **29**, 1137 (1984); University of São Paulo Report No. IFUSP/P-404 (1983).
- <sup>19</sup>B. L. Berman, R. E. Pywell, M. N. Thompson, K. G. McNeill, J. W. Jury, and J. G. Woodworth, *Bull. Am. Phys. Soc.* **31**, 855 (1986).